journal of the mechanical behavior of biomedical materials 103 (2020) 103555

Contents lists available at ScienceDirect

Journal of the Mechanical Behavior of Biomedical Materials

journal homepage: http://www.elsevier.com/locate/jmbbm

Manufacture and characteristics of HA-Electrodeposited polylactic acid/polyvinyl alcohol biodegradable braided scaffolds

Ting-Ting Li [a,b], Yi Zhang [a], Lei Ling [a], Mei-Chen Lin [c,d], Yunlong Wang [e], Liwei Wu [a,b,**], Jia-Horng Lin [f,a,b,c,d,g,h,***], Ching-Wen Lou [a,b,f,g,i,j,*]

[a] Innovation Platform of Intelligent and Energy-Saving Textiles, School of Textile Science and Engineering, Tiangong University, Tianjin, 300387, China
[b] Tianjin and Ministry of Education Key Laboratory for Advanced Textile Composite Materials, Tiangong University, Tianjin, 300387, China
[c] School of Chinese Medicine, China Medical University, Taichung, 40402, Taiwan
[d] Laboratory of Fiber Application and Manufacturing, Department of Fiber and Composite Materials, Feng Chia University, Taichung, 40724, Taiwan
[e] College of Textiles and Clothing, Xinjiang University, Xinjiang, 830046, China
[f] Fujian Key Laboratory of Novel Functional Fibers and Materials, Minjiang University, Fuzhou, 350108, China
[g] College of Textile and Clothing, Qingdao University, Shandong, 266071, China
[h] Department of Fashion Design, Asia University, Taichung, 41354, Taiwan
[i] Department of Bioinformatics and Medical Engineering, Asia University, Taichung, 41354, Taiwan
[j] Department of Medical Research, China Medical University Hospital, China Medical University, Taichung, 40402, Taiwan

ARTICLE INFO

Keywords:
Polylactic acid (PLA) filaments
Polyvinyl alcohol (PVA) filaments
Braids
Electrodeposition
Simulated body fluid

ABSTRACT

This study proposes the braided bone scaffolds. First, biologically degradable polylactic acid (PLA) filaments and polyvinyl alcohol (PVA) filaments are plied into composite yarns using a doubling and twisting machine. The composite yarns are tested to determine the optimal mechanical properties and a stabilized morphology. The PLA/PVA composite yarns are then braided into bone scaffolds, during which the optimal braiding process parameters and yarn ratio are determined. Based on the surface observation and tensile strength, a gear ratio of 45:45 provides the tubular braids with an optimal morphology and porosity that meet the biological requirements. When the PLA/PVA ratio is 3:1, the braids exhibit the maximum tensile properties and the most stable space structure. Furthermore, to make the braids a bioactive material with surface active sites, the braids are coated with hydroxyapatite (HA) by electrodeposition. The resulting HA-electrodeposited bone scaffolds are tested by *in vitro* biological experiments using a scanning electronic microscope (SEM), *energy dispersive x-ray analysis(EDAX), X-ray Diffraction(XRD), and Fourier transform infrared spectroscopy(*FT-IR), thereby examining their characteristics and microstructure. Results suggest that HA is electrodeposited over the bone scaffolds successfully. The immersion in simulated body fluid (SBF) is proven to contribute a good *in vitro* bioactivity to bone scaffolds. As a result, bone scaffolds are a good candidate for the application in the cancellous bone repairing field.

1. Introduction

In recent years, bone tissue engineering helps the impaired bones to heal. The impaired bone with a lower level of damage can self-heal (Nandi et al., 2010), but an artificial aid is needed for the impaired bones that are severely damaged. Due to the special request of the applying environment, good biocompatibility, biodegradability, spatial morphological structure, and mechanical strength are required by bone scaffolds. So far, metallic, ceramic, polymer (Serra et al., 2015) and composite materials (Araújo et al., 2015; Lin et al., 2016) have been

* Corresponding author. Innovation Platform of Intelligent and Energy-Saving Textiles, School of Textile Science and Engineering, Tiangong University, Tianjin, 300387, China.
** Corresponding author. Innovation Platform of Intelligent and Energy-Saving Textiles, School of Textile Science and Engineering, Tiangong University, Tianjin, 300387, China.
*** Corresponding author. Innovation Platform of Intelligent and Energy-Saving Textiles, School of Textile Science and Engineering, Tiangong University, Tianjin, 300387, China.
E-mail addresses: wuliwei@tjpu.edu.cn (L. Wu), jhlin@fcu.edu.tw (J.-H. Lin), cwlou@asia.edu.tw (C.-W. Lou).

https://doi.org/10.1016/j.jmbbm.2019.103555
Received 12 July 2019; Received in revised form 25 November 2019; Accepted 25 November 2019
Available online 27 November 2019

used for the production of bone scaffolds. Among the calcium phosphates in the nature, hydroxyapatite ($Ca_{10}(PO_4)_6(OH)_2$, HA) has comparable constituent components to the human hard tissue (Sopyan et al., 2007). Due to having good biocompatibility, osteoconduction, wettability (Suh and Matthew, 2000; Tan et al., 2011), and bone regeneration (Lee et al., 2008; Rodriguez et al., 2013), HA can adsorb calcium ions in the bodily fluid (Liu et al., 2006; Zhao et al., 2002) and serve as fillers of biopolymer-based composites for bone repair (Hu et al., 2014; Roh et al., 2016).

The biomaterial bone scaffolds are required to satisfy the physical, chemical and bioactive properties as they simulate the organic and mineral components of the human bones, for which the chemical constitution and mechanical strength at the tissue level are both necessary (Kashte et al., 2017). Polyvinyl alcohol (PVA) is one of the most widely used polymers in biomedical field. PVA polymer exhibit low mechanical strength when used in bone scaffolds (Liu et al., 2013). In order to make up this defect, it is generally possible to incorporate nanoparticles, such as carbon carbon nano onions (Grande Tovar et al., 2019) or graphene oxide (Pandele et al., 2014), or crosslinked biogels such as silicate gels (Pang et al., 2019). Polylactic acid (PLA) fulfills a suitable degradation rate and mechanical properties that close to the native tissue and absence of cytotoxicity (Trachtenberg et al., 2014). Therefore, it has also been approved as a biomedical material by the Food and Drug Administration (FDA) (Germain et al., 2018). After long-term implantation of PLA in mice, the inflammation caused by PLA during the degradation process is very mild and has little effect on the regeneration of whole bone tissue (Pistner et al., 1993). This mild inflammation can also be inhibited by incorporation of calcium phosphates on regeneration (Rogina et al., 2016). PLA filaments exhibit higher mechanical property than PVA, and thus are used as the reinforcement for PVA braids.

Textile structure has natural flexibility and aspect ratio. Among them, braids have longitudinal high tensile properties and a reticular structure formed by interlaced yarns with uniform and continuous pores. The manipulated manufacture makes textile structure commonly used or compounded with other biomedical polymers to produce artificial nerve conduit, artificial blood vessels and artificial bone scaffold in the tissue engineering field (Li et al., 2019b). When composed of different mechanical parameters, braids can acquire various morphological structures. A combination of a mandrel and yarns can form hollow braids. Furthermore, braids can also be repetitively fed into a braiding machine, which enable fibers or yarns being braided and overlapped to form bone scaffolds with multiple layers and adjustable diameters (Ling et al., 2019; Lou et al., 2012). Therefore, in this study, PLA/PVA composite yarns that feature good biocompatibility are used to form braids. Next, the braids are coated with a low crystalline HA layer using electrodeposition, thereby simulating the structure of the human bone and providing bone scaffolds with osteoconduction. This design fully takes advantages of composite yarns and HA, and makes a contribution to tissue engineering in terms of artificial bone scaffolds.

2. Experimental

2.1. Materials

Polyvinyl alcohol (PLA) filaments have a specification of 50D/36F. Polyvinyl alcohol (PVA) filaments have a specification of 38D/6F. Titanium (Ti) rods have a concentration of 99.6%, a diameter of 3 mm, and a length of 5 cm.

2.2. Preparation of PLA/PVA composite yarns

A winder (JWK2761A, China) and a doubling and twisting machine (DSTw-01B–C, China) are used to twist and ply the PVA and PLA filaments to form composite yarns. The parameters for the latter machines: yarn count of 22.5 tex, seven twist factors of 137, 142, 147, 152, 157, 162, and 167, a discharge rate of 25 m/min, and spindle speed of 8000 r/min. The composite yarns are thermally treated in a hot air circulation oven (101–4, China) at 90, 100, or 110 °C for 20, 30, or 40 min in order to set twists.

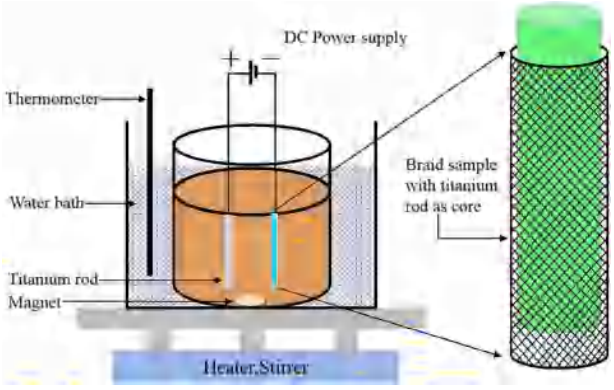

Fig. 1. Schematic diagram of electrodeposition of HA on PLA/PVA braids.

2.3. Preparation of PLA/PVA braids

PLA/PVA composite yarns that are composed of yarn ratios of 1:0, 3:1, 1:1, 1:3, and 0:1 are made into PLA/PVA braids using braiding machine with a gear ratio of take-up gear to braid gear being 50:40, 45:40, 40:40, 34:40, and 34:50.

2.4. HA-electrodeposited braided scaffolds

A titanium (Ti) rod (length: 50 mm, diameter: 3 mm, purification: 99.6%, China) is first polished for a sleek surface via the mechanical grinding with 400–1200 mesh sandpapers. Next, the rod is separately ultrasonic processed with absolute alcohol, acetone, and deionized water for 1 h (h), after which it is dried at 70 °C for 1 h in order to remove the greases and impurities. The composite yarns composed of PVA/PLA ratio being 1:3 are coiled surrounding a winder on a 16-spindle braiding machine. The Ti rod is used as the mandrel surrounding which the yarns are braided. With a specified gear ratio of 45:40, the composite yarns are braided in five layers, forming 4-mm-diameter mandrel-inserted braids.

Fig. 1 shows the electrodeposition process of HA over the braids. A braid inserted with the mandrel is immersed in an electrolyte solution composed of 0.05 M $CaCl_2$, 0.03 M KH_2PO_4, 0.05 M KCl, and a Ca/P ratio being 1.67. Triggered by an electric field, calcium ions and phosphate ions separately move toward the cathode and anode, during which Ca^{2+} and PO_4^{3-} ions are constantly adsorbed by the braids to coat an HA layer. PVA/PLA braids serve as the matrices for HA. The auto range DC power supply has an accuracy of 0.1 mV/mA and 60 V/15 A/360 W (IT6942A, ITECH, Japan) in a constant current mode, and the current density is 5.0 mA/cm^2. The temperature of heating in a water bath is 60 °C and the magnetic stirrer operates at a rotation rate of 120 rpm. During the electrodeposition of HA, a Ti rod is used as the anode and another T rod enwrapped by a 5-layered braid is used as the cathode. The electrodes are 20 mm apart. After deposition time of 90 min, the Ti rod is removed from the HA-deposited bone scaffold. The electrodeposition parameters have been optimized in our previous study (Li et al., 2019a; Li et al., 2019c).

2.5. Characterizations

2.5.1. Tensile properties of composite yarns

As specified in GB/T3916-2013, a single fiber strength machine (YG020, YUANMORE, China) is used to measure the tensile strength of composite yarns made of seven twist factors. The distance between

Table 1
Mixture ratio of simulated body fluid.

Elements	Weight
NaCl	7.996 g
$NaHCO_3$	0.350 g
KCl	0.224 g
$K_2HPO_4{\cdot}3H_2O$	0.228 g
$MgCl_2{\cdot}6H_2O$	0.305 g
1 M-HCl	40 ml
$CaCl_2$	0.440 g
Na_2SO_4	0.071 g
$NH_2C(CH_2OH)_3$	6.057 g

gauges is 250 mm, and the tensile rate is 250 mm/min. Ten samples for each specification are used.

2.5.2. Morphology and mechanical properties of braids

The surface of braids made of different gear ratio is observed at a magnification of 10x using a stereomicroscope (SMZ-10A, Nikon Instruments Co., Ltd, Japan), during which the diameter and braiding angle are recorded. As specified in ASTM D5034, the tensile strength of braids is evaluated at a tensile rate of 300 mm/min using a universal strength testing machine (HT-2402, HongTa Instrument, Taiwan) in terms of five PVA/PLA ratios. The distance between gauges is 75 mm. Five samples for each specification are used.

2.5.3. Characterizations of electrodeposited scaffolds

An Ion Sputtering Instrument (Blatc SCD005, BAL-TEC, US) is used to spur a layer of platinum over the samples. A scanning electron microscope (SEM, Germany) equipped with an accelerating 5000 voltage is used to observe the micro-structure of HA surface. According to ASTM D6641M-09, compression property is measured by Universal Strength Testing Machine (HT-2402, Hongta instrument, Taiwan) attached with 2 kN sensor at crosshead speed of 2 mm/min. The sample is a cylinder with a length of 20 mm and a diameter of 4 mm. Fitted with an energy dispersive x-ray analysis (EDAX EDS, Octane Super, US), a field emission scanning electron microscope (FE-SEM, Gemini SEM500, Germany) is used to observe the morphology of the coated HA lay over the bone scaffolds, after which the element composition of the HA layer is analyzed. Furthermore, the chemical bonds of HA coating is investigated with a resolution being 0.5 cm^{-1} at frequency of 400–4000 cm^{-1} using a Fourier transform infrared spectroscope (FTIR, Nicolet iS50, Thermo Fisher Scientific, Waltham, MA, US). Moreover, the phase composition of HA coating is investigated at CuKα radiation $\lambda = 1.5405$ with 2θ being 20–45° using an X-ray diffraction (XRD, D8 Discover, Bruker, Karlsruhe, Germany). Before the FTIR and XRD tests, samples are kept in an oven containing copper sulphate for 12 h to avoid the inferences of water.

2.5.4. Bioactivity test of HA-Electrodeposited scaffolds

Bioactivity is deemed as a chemical synthesis with the human hard tissue when scaffolds are grafted into the human body. An acellular fluid containing ions with concentrations that is similar to blood plasma (*i.e.* simulated body fluid, SBF) is used in the *in vitro* experiments. Comparing to HA, SBF is thermodynamically supersaturated. Bioactive materials that have surface active sites for HA nucleation are immersed in an SBF, the surface will form an apatite layer (Kokubo and Takadama, 2006). Khalili et al. (2017) and Zhang et al. (2018) conducted biomineralization experiments to examine the surface bioactivity and biomineralization property of PVA/PLA bone scaffolds. HA-deposited bone scaffolds are immersed in a protein- and cell-free SBF that is formulated referring to Kokopo method (Oyane et al., 2003) for seven days. The ingredients of 1 L of SBF are introduced in Table 1. Under an environment at 37 °C, 1 M HCl is added to SBF in order to obtain a pH value of 7.4, and the SBF volume required by samples is computed using the equation as follows (Muller and Muller, 2006).

$$S/V = 0.05\ cm^{-1} \quad (1)$$

where S is the exposed area and V is the volume of SBF.

SBF is changed on a daily basis in order to stabilize the ion concentration and pH value. One batch of braids are removed after 1-, 3-, 5-, and 7-day SBF immersion and then dried in a vacuum drying oven at 70 °C for 1 h to serve as the control group. The other batch of braids treated with the aforementioned process is electrodeposited with HA to serve as the experimental groups. The SEM images are photographed in order to observe the differences in the morphology.

3. Results and discussion

3.1. Tensile properties of composites yarns

Fig. 2 (a) shows the breaking strength of the composite yarns as related to the twist factor. When the twist factor of 137 rises at increments of 5, the composites yarns have an average breaking strength that increases by degrees. With a twist factor being 152, the maximum breaking strength occurs, after which it descends gradually. The results indicate that the critical twist factor of composite yarns is 152 (32 T/10 cm).

Fig. 2 (b) shows the test results of the heat setting effect of twists. A short heating time and a suitable heating temperature exaggerate the

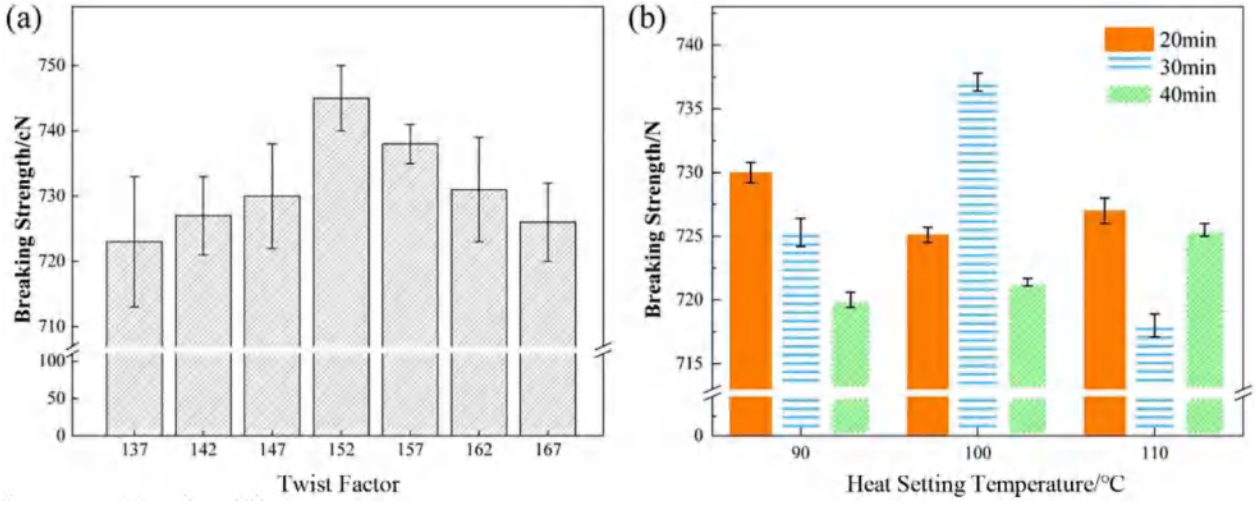

Fig. 2. Breaking strength of composite yarns as related to a) the twist factor and b) heat setting for twists.

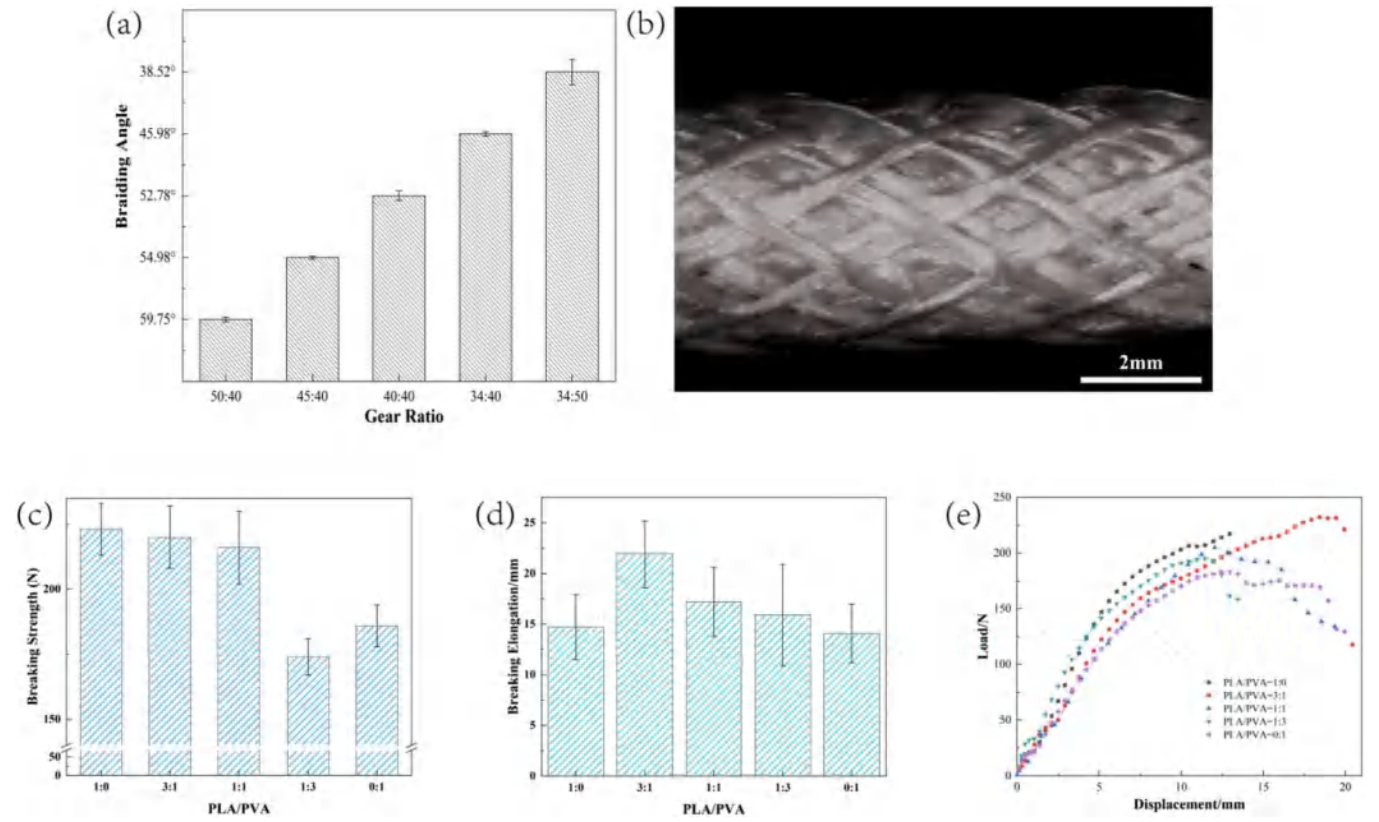

Fig. 3. a) Braiding angles of braids as related to gear ratio; b) stereomicroscopic image (× 10) of composite yarn made of a take-up gear/braid gear ratio of 45:40; and c) breaking strength, d) breaking elongation, and e) load-displacement curves of braids as related to the PLA/PVA mixture ratio.

Table 2
Diameter of braided scaffolds as related to gear ratio.

Take-up gear :Braid gear	Gear Ratio	Average Diameter /mm	Coefficient of Variation (CV)
50:40	1.25	2.96	0.027
45:40	1.125	3.05	0.015
40:40	1	3.10	0.015
34:40	0.85	3.41	0.029
34:50	0.68	3.18	0.060

molecular movement, during which the molecular chains are unchained and subsequently molecules are rearranged. This process stabilizes the formation of yarns. By contrast, an excessive temperature or heating time adversely affects the whole structure of yarns, which in turn causes the strength loss. To sum up, the optimal heat setting for twists of composite yarns is to proceed at 100°Cfor 30 min.

3.2. Characterizations and properties of braids

Fig. 3 (a) indicates the braiding angles of braids are 59.75°, 54.98°, 52.78°, 45.98°, and 38.52° when the ratio of the take-up gear to the braid gear are 50:40, 45:40, 40:40, 34:40, and 34:50, respectively. Table 2 shows the diameter of the braids as related to the gear ratio. When the gear ratio decreases, the diameter increases by degrees. In particular, with a gear ratio of 45:40, the braids have a stabilized structure with the lowest coefficient of variation in the diameter. Fig. 3 (b) shows the stereomicroscopic image of PLA/PVA braids that are made of a gear ratio being 45:40 and not removed from Ti rod. Based on the braiding angle, diameter, morphology and gear ratio (45:40), the braids are more mechanically supportive and stabilized. Therefore, the specified gear ratio is used for subsequent discussions.

Fig. 3 (c, d) shows that the breaking strength is proportional to the content of PLA filaments, except for the PLA/PVA ratios of 1:3 and 0:1. Pure PVA braids made of 0:1 PLA/PVA yarns have greater breaking strength than braids composed of 1:3 PLA/PVA composite yarn because of different morphology and structures of two composite yarns. During set twisting or braiding, the deformation occurs, but this deformation process is asynchronized for PLA and PVA filaments because both of which have different elastic modulus. Therefore, during tensile test, the loading of PLA and PVA filament among plied yarns occurs not simultaneously which results in the fact that PLA/PVA plied braid has lower tensile strength than pure PVA braid. Moreover, the coefficient of variation of tensile strength is smaller for pure PVA braid compared to other braids made of plied yarns. With the closer mixture ratio of PLA and PVA (for 1:1 PLA/PVA composite braid), the structure of twisting composite yarns is more complex, its coefficient of variation becomes bigger, and tensile strength changes more unstable. The breaking strength of the PLA/PVA ratio of 3:1 is 25% higher than that of the PLA/PVA ratio of 0:1. Moreover, the elongation at break of PLA/PVA ratio of 3:1 is only increased by 11% compared with the pure PLA braid, but the former is 163% higher than pure PVA braid. This result indicates that the PLA filament significantly reinforces the mechanical property of composite braid.

Fig. 3 (d, e) shows the breaking elongation and load-displacement curves of braid as related to the PLA/PVA mixture ratio. The other four PLA/PVA ratios provide the braids with comparable breaking elongation, exclusive of 3:1 that provides the braids with considerably higher breaking elongation and relatively higher tensile strength with a small coefficient of variation. Namely, a PLA/PVA ratio of 3:1 realizes the reproducibility.

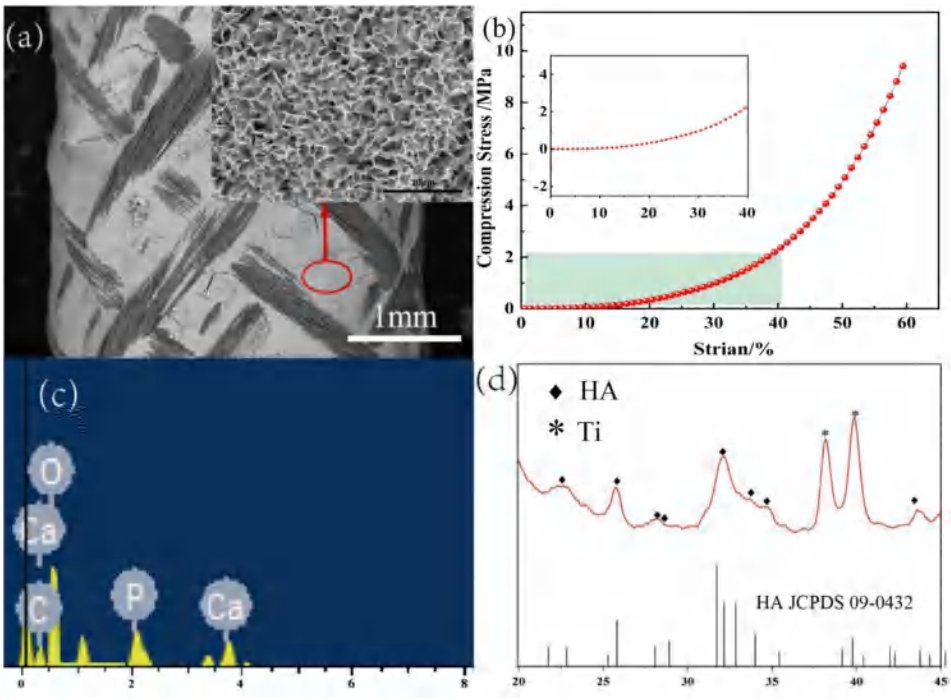

Fig. 4. a) SEM images of HA-electrodeposited braided scaffolds; b) Stress-strain curve for HA-electrodeposited braided scaffolds under compression; c) EDS and d) XRD charts of HA-electrodeposited braided scaffolds.

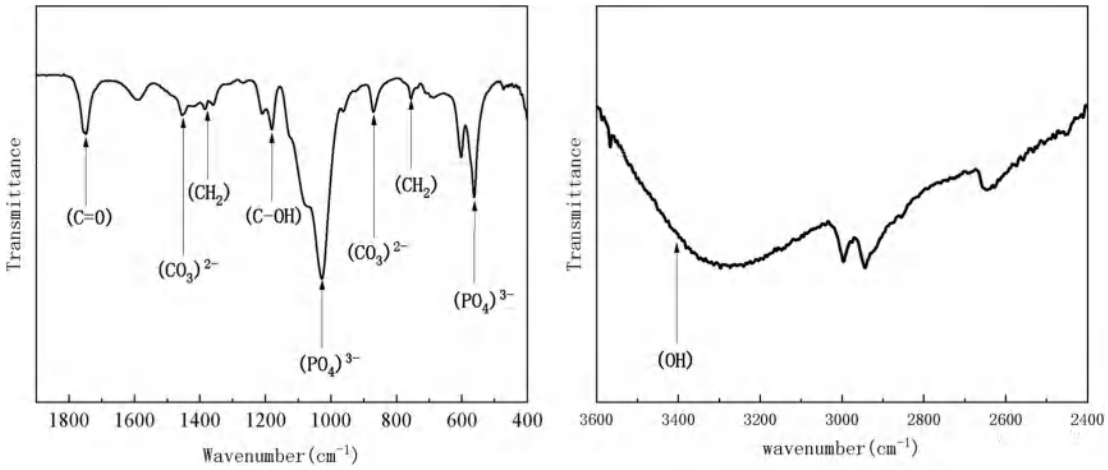

Fig. 5. FTIR spectra of deposited HA layer of braided scaffolds.

3.3. Characterizations of braid scaffolds electrodeposited with an HA layer

Fig. 4 (a) shows the SEM images (5000 ×) of HA-coating bone scaffolds by electrodeposition. The HA crystals appear to be microporous and a stratified structure, proving that a current density of 5.0mA/cm2 generates a uniform and dense HA coating layer. Fig. 4 (b) shows the compression stress-strain of PLA/PVA bone scaffolds. At compression strain of 60%, our fabricated bone scaffold reaches the compression stress up to 9.5 MPa. This value lies in-between the strength of human cancellous bone (4–12 MPa), and is much higher than that of bone scaffolds made by chitosan/multiphasic calcium phosphate (420 kPa) and 3D-printed PLA scaffolds (7.6 ± 2.3 MPa) (Mohammadi et al., 2016; Song et al., 2018). Based on the elemental composition of HA coating layer characterized by EDS (Fig. 4 (c)), the Ca/P atomic ratio is 1.70, which resembles that of stoichiometric ratio of calcium and phosphorus (1.67) of HA. Fig. 4 (d) shows the XRD spectra of HA coating over the bone scaffolds where the diffraction peak reflects the amount of HA deposition and the degree of crystallization. Based on the consistent diffraction peak of HA diffraction file (#09–0432) in the ICDD database, it is proven that HA crystals are successfully deposited over the bone scaffolds. The diffraction peaks with the corresponding crystal plane are 25.9° (002), 31.8° (211), 32.2° (112), 32.9° (300), and 39.8° (310). Fig. 5 shows the infrared spectrum of HA coating that is electrodeposited over the bone scaffolds. The characteristic peaks at 567 and 603 cm^{-1} correspond to the bending vibration of PO_4^{3-}; the characteristic peaks at 900-1200 cm^{-1} correspond to the symmetric and asymmetric stretching vibrations of the PO_4^{3-} ions, and the low characteristic peak at 3571 cm^{-1} is HA's hydroxyl. Moreover, the characteristic peaks at 870 cm^{-1} and 1415-1458 cm^{-1} means the presence of CO_3^{2-}, suggesting the presence of B- or A-type carbonated hydroxyapatite (CHA). A small amount of PO_4^{3-} is replaced by CO_3^{2-} that is formed as a result of carbon dioxide being dissolved in water (Fathyunes and Khalil-Allafi, 2018). In addition, it has been proven that CHA is a crucial factor to synthesis of

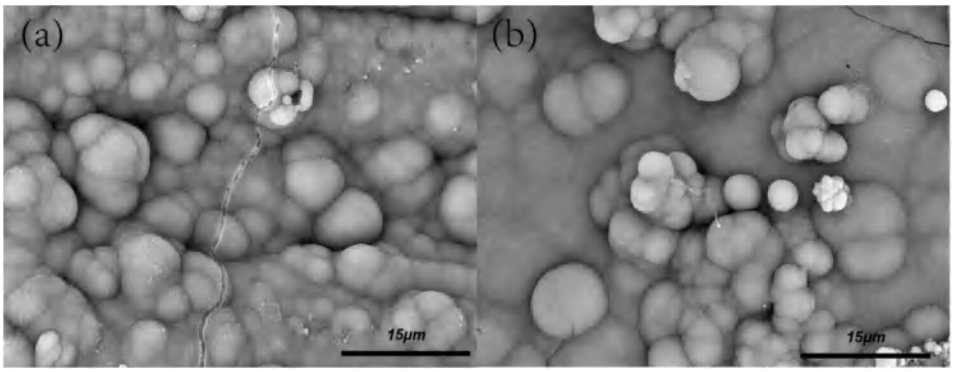

Fig. 6. SEM images of bone scaffolds that are deposited with HA in an SBF for a) 3 and b) 7 days.

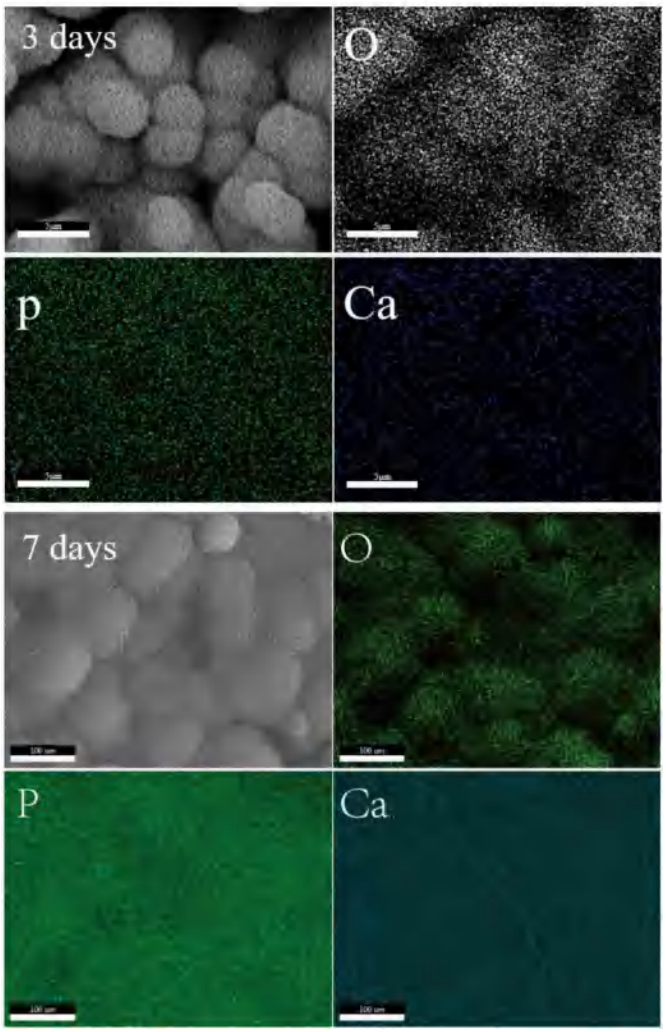

Fig. 7. EDS mapping of bone scaffolds immersed in an SBF for three and seven days.

natural bones (Anandan et al., 2019). Serving as the matrices for electrodeposition, PVA/PLA braids also show some characteristic peaks, such as carboxyl of PLA at 1185 cm $^{-1}$, methyl of PLA/PVA composite yarns at 1457 and 754 cm $^{-1}$, carbon-oxygen double bond of PLA at 1744 cm^{-1}, and the interior hydrogen bond at 3230–3550 cm $^{-1}$ (Li et al., 2019a).

3.4. In vitro biomineralization

In vitro biomineralization property is the chemical bonding ability of the human hard tissue to form bones. Fig. 6 shows the SEM images of HA-deposited bone scaffolds that are immersed in the SBF for 3 and 7 days. It is found that flake-like electroposited HA microporous structure is firstly damaged, and subsequently, spherical HA crystal particles are then precipitated. With a longer length of time, more and more spherical particles of HA are found over the HA coating layer. Comparatively, surficial spherical HA crystals of 7-day immersed scaffolds become more rounded and more complete than that of 3-day immersed scaffolds, which suggests good *in vitro* biomineralization property. In Fig. 7, the EDS spectrum of the braided scaffolds is mapped after 3- and 7-day immersion in the SBF solution. After 3-day immersion, the HA flaky microporous structure coating gradually disappeared, and spherical particles were precipitated, and the particles became larger as the soaking time increased to 7days. The EDS mapping indicates a coating layer rich in HA over the bone scaffolds accompanied with evenly distributed Ca and P elements immersed for 3 and 7 days. In contrast, the HA-deposited bone scaffold after 7 days of SBF immersion showed larger and rounder HA globular particles, and the distribution of Ca and P elements became more uniform, indicating that HA-deposited bone scaffolds can provide good *in vitro* biological activity and biomineralization property.

4. Conclusion

PLA/PVA composite braided scaffolds that are electrodeposited with a hydroxyapatite layer exhibit a strengthened bioactivity. The mechanical properties of PLA/PVA composites yarns are evaluated, while the composite braids and HA-coated bone scaffolds are observed for micro-structure and evaluated for *in vitro* bioactivity. The optimal critical twist factor of PLA/PVA composite yarns is 152 (32 T/10 cm) and the optimal thermal treatment is at 100 °C for 30 min. With a ratio of the take-up gear to the braid gear being 45:40, the braids have a stabilized structure. Moreover, a PLA/PVA ratio of 3:1 provides the braids with the maximum mechanical properties in terms of breaking strength and elongation. Moreover, the HA-electrodeposited bone scaffolds demonstrate a good *in vitro* bioactivity in a simulated body fluid.

Declaration of competing interest

The authors declare no conflict of interest.

Acknowledgements

This work is supported by the Natural Science Foundation of Tianjin (18JCQNJC03400), the Natural Science Foundation of Fujian (2018J01504, 2018J01505) and the National Natural Science

Foundation of China (grant number 11702187). This study is also supported by the Opening Project of Green Dyeing and Finishing Engineering Research Center of Fujian University (2017001A, 2017001B, and 2017002B) and the Program for Innovative Research Team in University of Tianjin (TD13-5043).

Appendix A. Supplementary data

Supplementary data to this article can be found online at https://doi.org/10.1016/j.jmbbm.2019.103555.

References

Anandan, D., Madhumathi, G., Nambiraj, N.A., Jaiswal, A.K., 2019. Gum based 3D composite scaffolds for bone tissue engineering applications. Carbohydr. Polym. 214, 62–70.

Araújo, A.P.C., Venturelli, B.C., Santos, M.C.B., Gardinal, R., Cônsolo, N.R.B., Calomeni, G.D., Freitas, J.E., Barletta, R.V., Gandra, J.R., Paiva, P.G., Rennó, F.P., 2015. Chitosan affects total nutrient digestion and ruminal fermentation in Nellore steers. Anim. Feed Sci. Technol. 206, 114–118.

Fathyunes, L., Khalil-Allafi, J., 2018. Effect of employing ultrasonic waves during pulse electrochemical deposition on the characteristics and biocompatibility of calcium phosphate coatings. Ultrason. Sonochem. 42, 293–302.

Germain, L., Fuentes, C.A., van Vuure, A.W., des Rieux, A., Dupont-Gillain, C., 2018. 3D-printed biodegradable gyroid scaffolds for tissue engineering applications. Mater. Des. 151, 113–122.

Grande Tovar, C.D., Castro, J.I., Valencia, C.H., Navia Porras, D.P., Mina Hernandez, J. H., Valencia, M.E., Velasquez, J.D., Chaur, M.N., 2019. Preparation of chitosan/poly (vinyl alcohol) nanocomposite films incorporated with oxidized carbon nano-onions (Multi-Layer fullerenes) for tissue-engineering applications. Biomolecules 9.

Hu, X., Shen, H., Yang, F., Liang, X., Wang, S., Wu, D., 2014. Modified composite microspheres of hydroxyapatite and poly(lactide-co-glycolide) as an injectable scaffold. Appl. Surf. Sci. 292, 764–772.

Kashte, S., Jaiswal, A.K., Kadam, S., 2017. Artificial bone via bone tissue engineering: current scenario and challenges. Tissue Eng. Regen. Med. 14, 1–14.

Khalili, V., Khalil-Allafi, J., Frenzel, J., Eggeler, G., 2017. Bioactivity and electrochemical behavior of hydroxyapatite-silicon-multi walled carbon nano-tubes composite coatings synthesized by EPD on NiTi alloys in simulated body fluid. Materials Science & Engineering C-Materials for Biological Applications 71, 473–482.

Kokubo, T., Takadama, H., 2006. How useful is SBF in predicting in vivo bone bioactivity? Biomaterials 27, 2907–2915.

Lee, J.B., Lee, S.H., Yu, S.M., Park, J.-C., Choi, J.B., Kim, J.K., 2008. PLGA scaffold incorporated with hydroxyapatite for cartilage regeneration. Surf. Coat. Technol. 202, 5757–5761.

Li, T.-T., Ling, L., Lin, M.-C., Jiang, Q., Lin, Q., Lin, J.-H., Lou, C.-W., 2019. Properties and mechanism of hydroxyapatite coating prepared by electrodeposition on a braid for biodegradable bone scaffolds. Nanomaterials 9.

Li, T.T., Ling, L., Lin, M.C., Jiang, Q., Lin, Q., Lou, C.W., Lin, J.H., 2019. Effects of ultrasonic treatment and current density on the properties of hydroxyapatite coating via electrodeposition and its in vitro biomineralization behavior. Mater Sci Eng C Mater Biol Appl 105, 110062.

Li, T.-T., Zhong, Y., Yan, M., Zhou, W., Xu, W., Huang, S.-Y., Sun, F., Lou, C.-W., Lin, J.-H., 2019. Synergistic effect and characterization of graphene/carbon nanotubes/polyvinyl alcohol/sodium alginate nanofibrous membranes formed using continuous needleless dynamic linear electrospinning. Nanomaterials 9.

Lin, W.-H., Yu, J., Chen, G., Tsai, W.-B., 2016. Fabrication of multi-biofunctional gelatin-based electrospun fibrous scaffolds for enhancement of osteogenesis of mesenchymal stem cells. Colloids Surfaces B Biointerfaces 138, 26–31.

Ling, L., Li, T.-T., Lin, M.-C., Jiang, Q., Ren, H.-T., Lou, C.-W., Lin, J.-H., 2019. Effect of hydrogen peroxide concentration on the nanostructure of hydroxyapatite coatings via ultrasonic-assisted electrodeposition. Mater. Lett. 126989.

Liu, H., Li, H., Cheng, W., Yang, Y., Zhu, M., Zhou, C., 2006. Novel injectable calcium phosphate/chitosan composites for bone substitute materials. Acta Biomater. 2, 557–565.

Liu, Y., Lim, J., Teoh, S.-H., 2013. Review: development of clinically relevant scaffolds for vascularised bone tissue engineering. Biotechnol. Adv. 31, 688–705.

Lou, C.-W., Yao, C.-H., Chen, Y.-S., Lu, C.-T., Chen, W.-C., Yen, K.-C., Lin, J.-H., 2012. PLA/beta-TCP complex tubes: the mechanical properties and applications of artificial bone. J. Biomater. Sci. Polym. Ed. 23, 1701–1712.

Mohammadi, Z., Mesgar, A.S.-M., Rasouli-Disfani, F., 2016. Reinforcement of freeze-dried chitosan scaffolds with multiphasic calcium phosphate short fibers. J. Mech. Behav. Biomed. Mater. 61, 590–599.

Muller, L., Muller, F.A., 2006. Preparation of SBF with different HCO3- content and its influence on the composition of biomimetic apatites. Acta Biomater. 2, 181–189.

Nandi, S.K., Roy, S., Mukherjee, P., Kundu, B., De, D.K., Basu, D., 2010. Orthopaedic applications of bone graft & graft substitutes: a review. Indian J. Med. Res. 132, 15–30.

Oyane, A., Kim, H.M., Furuya, T., Kokubo, T., Miyazaki, T., Nakamura, T., 2003. Preparation and assessment of revised simulated body fluids. J. Biomed. Mater. Res. A 65A, 188–195.

Pandele, A.M., Ionita, M., Crica, L., Dinescu, S., Costache, M., Iovu, H., 2014. Synthesis, characterization, and in vitro studies of graphene oxide/chitosan-polyvinyl alcohol films. Carbohydr. Polym. 102, 813–820.

Pang, L., Shen, Y., Hu, H., Zeng, X., Huang, W., Gao, H., Wang, H., Wang, D., 2019. Chemically and physically cross-linked polyvinyl alcohol-borosilicate gel hybrid scaffolds for bone regeneration. Mater. Sci. Eng. C-Mater. Biol. Appl. 105.

Pistner, H., Gutwald, R., Ordung, R., Reuther, J., Muhling, J., 1993. Poly(L-lactide): a long-term degradation study in vivo. I. Biological results. Biomaterials 14, 671–677.

Rodriguez, G., Dias, J., d'Avila, M.A., Bartolo, P., 2013. Influence of hydroxyapatite on extruded 3D scaffolds. In: Bartolo, P., Fernandes, P. (Eds.), 3rd International Conference on Tissue Engineering, pp. 263–269.

Rogina, A., Pribolsan, L., Hanzek, A., Gomez-Estrada, L., Gallego Ferrer, G., Marijanovic, I., Ivankovic, M., Ivankovic, H., 2016. Macroporous poly(lactic acid) construct supporting the osteoinductive porous chitosan-based hydrogel for bone tissue engineering. Polymer 98, 172–181.

Roh, H.-S., Jung, S.-C., Kook, M.-S., Kim, B.-H., 2016. In vitro study of 3D PLGA/n-HAp/β-TCP composite scaffolds with etched oxygen plasma surface modification in bone tissue engineering. Appl. Surf. Sci. 388, 321–330.

Serra, I.R., Fradique, R., Vallejo, M.C.S., Correia, T.R., Miguel, S.P., Correia, I.J., 2015. Production and characterization of chitosan/gelatin/β-TCP scaffolds for improved bone tissue regeneration. Mater. Sci. Eng. C 55, 592–604.

Song, P., Zhou, C., Fan, H., Zhang, B., Pei, X., Fan, Y., Jiang, Q., Bao, R., Yang, Q., Dong, Z., Zhang, X., 2018. Novel 3D porous biocomposite scaffolds fabricated by fused deposition modeling and gas foaming combined technology. Compos. B Eng. 152, 151–159.

Sopyan, I., Mel, M., Ramesh, S., Khalid, K.A., 2007. Porous hydroxyapatite for artificial bone applications. Sci. Technol. Adv. Mater. 8, 116–123.

Suh, J.K.F., Matthew, H.W.T., 2000. Application of chitosan-based polysaccharide biomaterials in cartilage tissue engineering: a review. Biomaterials 21, 2589–2598.

Tan, N., Kou, Z., Ding, Y., Leng, Y., Liu, C., He, D., 2011. Novel substantial reductions in sintering temperatures for preparation of transparent hydroxyapatite bioceramics under ultrahigh pressure. Scr. Mater. 65, 819–822.

Trachtenberg, J.E., Mountziaris, P.M., Miller, J.S., Wettergreen, M., Kasper, F.K., Mikos, A.G., 2014. Open-source three-dimensional printing of biodegradable polymer scaffolds for tissue engineering. J. Biomed. Mater. Res. A 102, 4326–4335.

Zhang, H., Shi, X., Tian, A., Wang, L., Liu, C., 2018. Electrochemical properties of Ti3+ doped Ag-Ti nanotube arrays coated with hydroxyapatite. Appl. Surf. Sci. 436, 579–584.

Zhao, F., Yin, Y.J., Lu, W.W., Leong, J.C., Zhang, W.J., Zhang, J.Y., Zhang, M.F., Yao, K. D., 2002. Preparation and histological evaluation of biomimetic three-dimensional hydroxyapatite/chitosan-gelatin network composite scaffolds. Biomaterials 23, 3227–3234.